

Gravesoil derived postmortem interval using attenuated total reflectance-Fourier transform infrared spectroscopy and the influence of carrion associated fabric.

Phebie Watson^{1*}, Sulaf Assi¹ and Theresia Komang Ralebitso-Senior¹

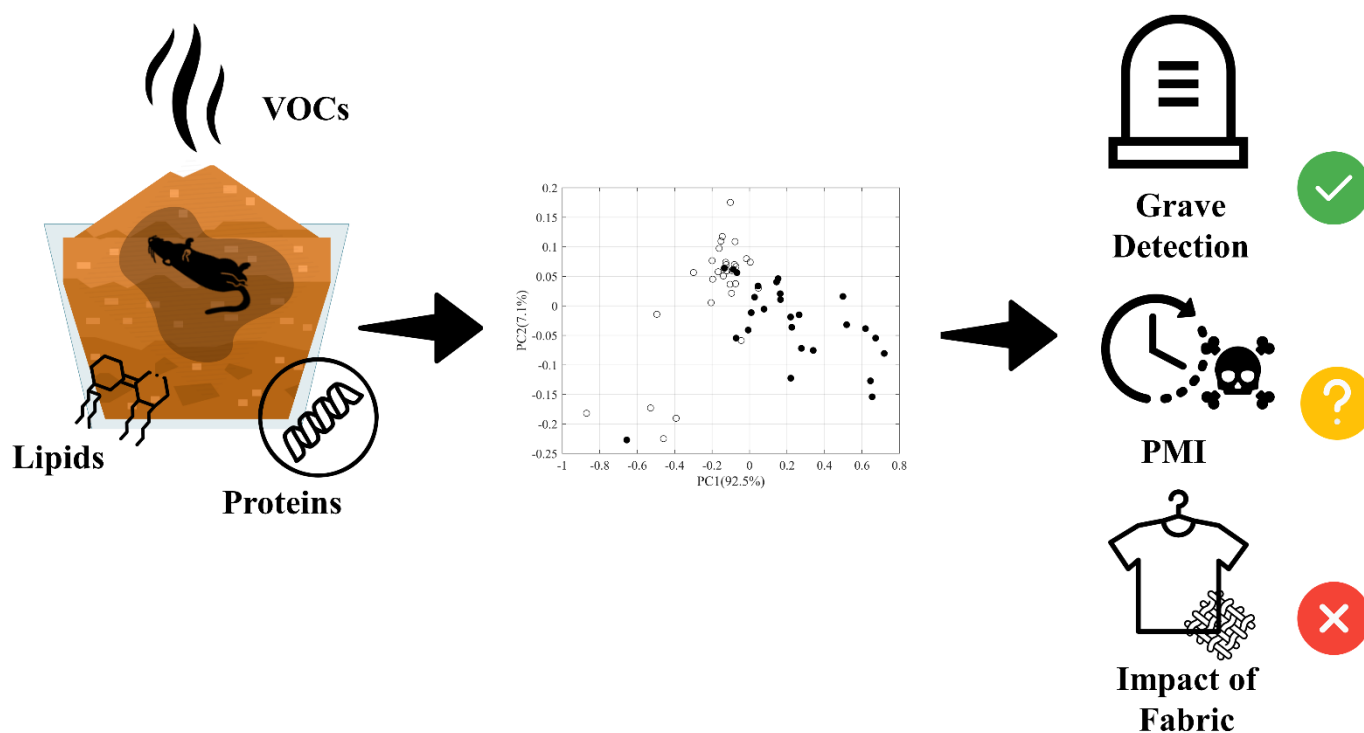
¹School of Pharmacy and Biomolecular Science, Liverpool John Moores University, Liverpool, L3 3AF United Kingdom

*Correspondence:

Phebie Watson

P.S.Watson@2019.ljmu.ac.uk

Graphical Abstract



Abstract

Establishing time elapsed for unattended death scenes is crucial in formulating a timeline of events facilitating death investigations. However, traditional postmortem interval (PMI) methods rely on visually evaluating physical atrophy and are closely influenced by both biotic and abiotic variables associated with carrion. During the bloat stage, carrion produce a characteristic landscape known as the cadaver decomposition island (CDI), through the propagation of fluids rich in decomposition by-products. Here, attenuated total reflectance-

Fourier transform infrared spectroscopy (ATR-FT-IR) was employed as a non-invasive, low input, low preparation interface for determining PMI from simulated *Mus musculus* burial gravesoil. Furthermore, understanding influences of environmental and inter-individual differences in gaining accurate PMI is important to validate, prior to implementation to enhance the current forensic toolkit. It is documented that the presence, type and weight of clothing interferes with progression through decomposition. The subsequent impacts of clothing material (cotton, polyester, viscose) on CDI footprint development will be reflected in the biological and chemical characteristics of this ecosystem. Principal component analysis (PCA) of the IR spectra showed two clusters of samples corresponding to control and gravesoil. PC loadings plot showed that the 3100 - 1000 cm^{-1} spectral range attributed for over 95% of the variance. Bands within this range are ascribed to the presence of lipids, proteins and volatile organic compounds (VOCs) as byproducts of mammalian decomposition. Overall, presence and fabric type impacted decomposition, spectral CDI detection and grave discrimination. This study questions the efficacy of proxy size and microcosm design in conducting applicable forensic research in lieu of taphonomy facilities or ethical constraints.

Keywords: postmortem interval, *Mus musculus*, clothing, ATR-FT-IR spectroscopy, clandestine grave

Introduction

Clothing are routinely used in forensic casework as they can provide evidence of laceration marks, fibre transfer and trace DNA (1–3). Recent work has highlighted the potential to track and identify patterns of decomposition in carrion-associated clothing as a tool to estimate postmortem interval (PMI) (4). Establishing the time elapsed for unattended death scenes is crucial for investigators to formulate a timeline of events that facilitates identification of the victim, possible suspects and corroboration of witness statements and alibis. Alongside tracking visual deterioration of the grave-associated textiles, anatomical accumulation and composition of decomposition fluids into cadaver clothing also assists in PMI estimation (5–7). During the active-bloat and purge stages, the carrion begins to release lipid-, protein- and carbohydrate-rich by-products of the degradation processes (8). Carter et al., (9) described the characteristic landscape that forms beneath a cadaver in a terrestrial environment as the cadaver decomposition island (CDI). This propagation of fluids, expelled by the cadaver post-rupture, permeates the surrounding environment and biogeochemically cycles. This surge of nutrients and enteric microorganisms into the local environment induces a succession of the soil physical and biochemical properties. Measurement of gravesoil physicochemical alterations such as

total extractable phosphorus and ninhydrin-reactive nitrogen (NRN) showed promise as a tool for the estimation of PMI (8,10). However, the novel tracking of cadaveric fluids into cotton and polyester, as described by both Ueland and Collins (6,11) infer that the natural migration of these measurable decomposition fluids into the surrounding environment may be subsequently impeded in both human and porcine models. It is also well understood that the presence, type and, weight of wrapping or clothing can delay or enhance progression through the decomposition stages (12,13). Furthermore, the subsequent impact of clothing on temporal and lateral development of CDI will be reflected in the soil's physicochemistry. Being able to locate and date corpse -related terrestrial samples is pertinent in scenarios where remains may have been exhumed, relocated or desiccated beyond taphonomic classification.

Attenuated total reflectance Fourier transform infrared (ATR-FT-IR) has been utilised for many forensic applications including identification of illicit substances, counterfeit pharmaceuticals, bodily fluid detection, and soil or fibre analysis (14–17). Gravesoil sampling is a non-invasive alternative of gaining PMI, thus ATR-FT-IR lends itself to the forensic tool kit as it is rapid, portable, and reproducible, requiring only a small aliquot of sample material with little preparation. ATR-FT-IR negates the need for labelling molecules within a mixed unknown sample as it relies on the absorbance of molecular vibrations of functional groups present and is; thus, highly beneficial (18). Considering these advantages, the present study used ATR-FT-IR spectroscopy to investigate temporal changes in gravesoil CDI formation of the taphonomically relevant *Mus musculus* analogue in the presence of fabrics sold as 100% cotton, polyester, and viscose. The current study aimed to investigate the viability of utilising ATR-FT-IR spectroscopy to distinguish gravesoil associated with murine carrion over a 6-month burial period. The hypotheses for the present work were that [1] murine decomposition gravesoil would be distinguished from the soil-only control and [2] the presence of different fabric wrapping around carrion would distinguish spectra obtained both temporally and between fabric type in a simulation burial setting. Murine models were chosen for this proof-of-concept study as they are deemed the most appropriate analogue for scale, replicability, and sufficient space in internal laboratory facilities for housing experimental microcosm. Similarly, due to current legal and ethical restrictions, access to taphonomy centres was not possible for work undertaken in the United Kingdom.

Materials and Methods

Twenty-four decomposition microcosms were set up and maintained in a dedicated laboratory fume hood (Sanber Ltd, Bolton, UK) at Liverpool John Moores University, Merseyside, UK for 170 days at ambient temperature (August 2021 – February 2022). Twelve frozen adult female domestic mice (*Mus musculus*) $\approx 18.2 \pm 1.21$ g, culled with an overdose of isoflurane, (ENVIGO, Oxfordshire, UK) were thawed fully prior to simulation burial at a depth of 5 cm in homogenised commercially sourced multipurpose topsoil (pH 5.5 – 6.0, Wickes, Northampton, UK). Microcosms were carried out in triplicate as follows: soil-only, cotton-only, polyester- only, viscose- only, unwrapped *M. musculus*, and those wrapped in cotton, polyester and viscose (Figure 1). The simulation microcosms 1 L polypropylene boxes (L17.2 x W11.3 x D7 cm) were further housed in sets of eight, in a random order, in polyethylene boxes (L60 x W40 x H27 cm), lined with a (~5 cm) layer of homogenised soil to encourage natural lateral flow of cadaveric fluid migration. The microcosm housing were watered once monthly, totalling 70 ml, to simulate the annual rainfall of Liverpool, Merseyside, United Kingdom (19). Internal microcosm moisture (%) and soil samples were taken on days 0, 4, 8, 16, 32, 50, 80, 110 and 170 through 1 cm diameter (n=12) perforations in the sides (Supplementary Figure 1). Aliquots of the homogenised composite soil samples (5 mg) were transferred into sterile 2.0 mL glass vials (Wheaton, New Jersey, USA) and stored at -20°C until spectroscopic analysis. The microcosms were destructively sampled on day 170. After removal of any mouse tissue, any remaining fabric retrieved was air-dried inside a fume cupboard at ambient temperature for 24 hours. Each of the dry fabric types were cut with sterile scissors into three 1 x 1 cm sections and stored in grip seal plastic pouches at -20°C until spectroscopic analysis.

Spectral measurements were made using the Cary 630 FT-IR Spectrometer (Agilent Technologies, CA, USA). Spectra of ground soil aliquots (1-2 mg) and pre-cut, dried fabric samples were recorded within a range of $4000 - 400 \text{ cm}^{-1}$, with a spectral resolution of 4 cm^{-1} averaged over 64 scans. Spectra were exported to MATLAB R2021b (The MathWorks Inc, MA, USA) for spectral interpretation and application of principal component analysis (PCA). In this respect, both PC scores- and loadings- plots were investigated. PC loadings highlighted key functional groups that had high variance in the model. Scores corresponding to samples collected on the same day were expected to cluster together and vice versa. To evaluate accuracy and precision of the model, scores were assessed for type I and II errors. Type I error

was encountered when scores of the same day/condition were not clustered together while type II error was seen when scores of soil grouped with a different PMI or microcosm treatment (20,21).

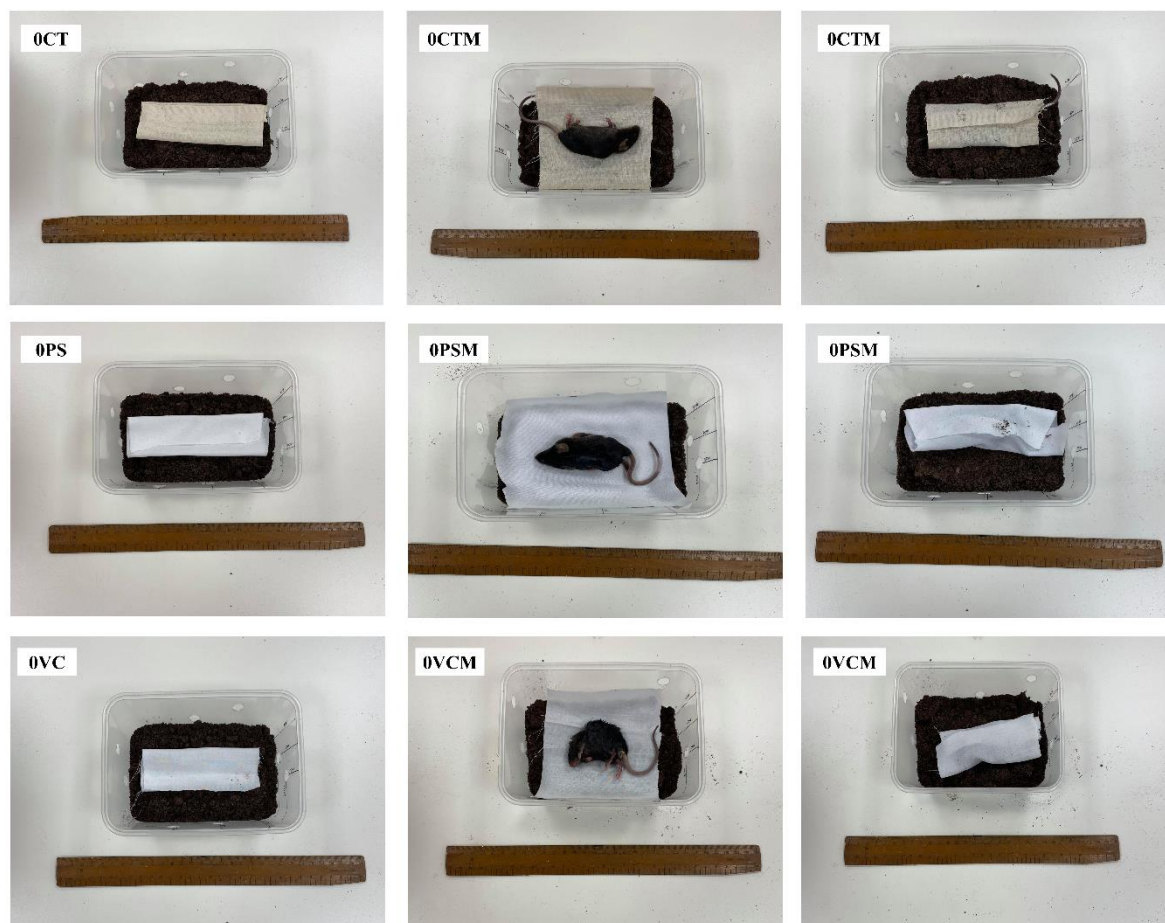


Figure 1. Microcosm set up day 0 (n=3): cotton (CT), polyester (PS), viscose (VC), cotton-wrapped *M. musculus* (CTM), polyester-wrapped *M. musculus* (PSM), viscose-wrapped *M. musculus* (VCM); buried at a depth of 5 cm in homogenized topsoil (pH 5.5 – 6.0).

Results and Discussion

Clothing, burial, and decomposition

Visually there were distinct differences in the degradation of each fabric, associated with burial or decomposing remains. Spectra obtained from the cotton pre- and post-burial showed reduced intensity of characteristic bands, namely the O-H, C-H and C-O stretching vibrations of cellulose at 3321 cm^{-1} , 2900 cm^{-1} and 1020 cm^{-1} (4,22), respectively (Figure 2). Additionally, minimal deterioration was observed in buried cotton-only samples 170 days post burial in absence of carrion (Figure 3A). This latter finding was consistent with the initial signs of cotton degradation reported to establish 149 to 269 days in situ deposition or burial (4). Ueland et al.,

(6,23) highlighted that burial environments and subsequent confounding factors such as texture and moisture accelerated visible and IR spectral signs of cotton deterioration. The present findings indicated enhanced cotton degradation when associated with decomposing murine remains, in a simulated burial context. On the contrary, previous reports showed that the interaction of cadaveric fluids substantially inhibited or slowed the degradation of cotton associated with domestic pig carcasses up to 12 months post-burial (23,24). The highly variable visual and spectral deterioration of buried cotton reported in the literature, irrespective of carrion, can be attributed to the influence of contemporary applied finishes on the fabric biodegradability (25,26)

Dissimilarly, viscose fabric could not be consistently retrieved 170 days post burial, independent of carrion, conferring rapid biodegradation recorded by Salar and Davrim, (2019) ex situ (22). Notably, small remnants of the experimental viscose fabric were preserved at the base of all carrion-associated graves (Figure 3B). Moreover, the regenerated cellulosic properties of viscose may have responded readily to microbial

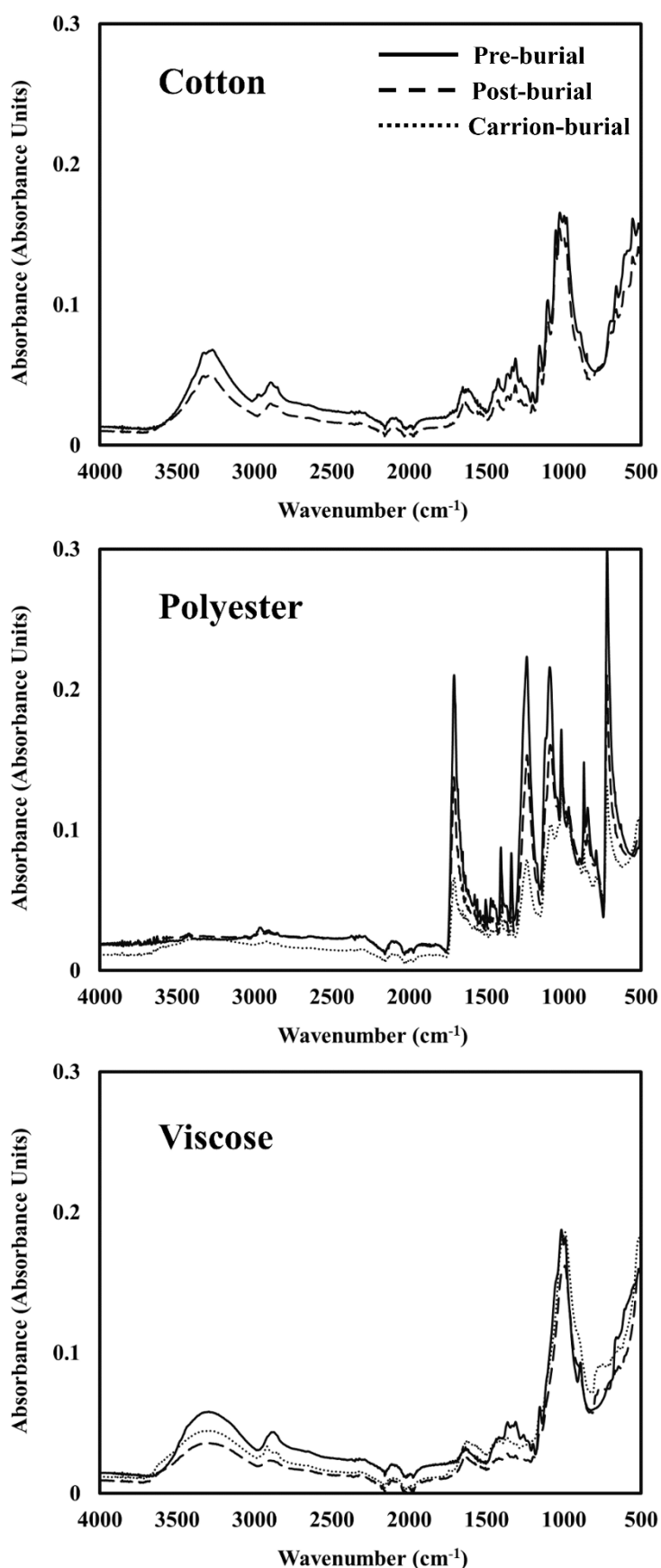


Figure 2. FTIR spectra of pre and post burial fabric samples over a range of 4000 – 500 cm^{-1} .

degradation when buried independently, in their highly amorphous, hydrophilic, and absorbent nature (22). On the other hand, preserved to a degree when in contact with cadaveric fluids as reported with porcine-associated cellulosic grave materials (5,6). Buried viscose spectra behaved similarly to buried cotton losing intensity at 3321 cm^{-1} , 2900 cm^{-1} , O-H and C-H stretching cellulose vibrations respectively (Figure 2). Additional characteristic functional groups at 720 , 1645 and 1540 cm^{-1} reduced in intensity when the fabric was buried, discordant with literature recording increased peak intensity at such markers associated with a post burial interval (PBI) of 120 days (22). Retrieved carrion-associated viscose indicated absorption of lipolysis and proteolysis products at 2920 cm^{-1} and 2850 cm^{-1} (CH_2 wagging) and $1650\text{-}1580\text{ cm}^{-1}$ (N-H bending) characteristic of amide I and II (11,15).

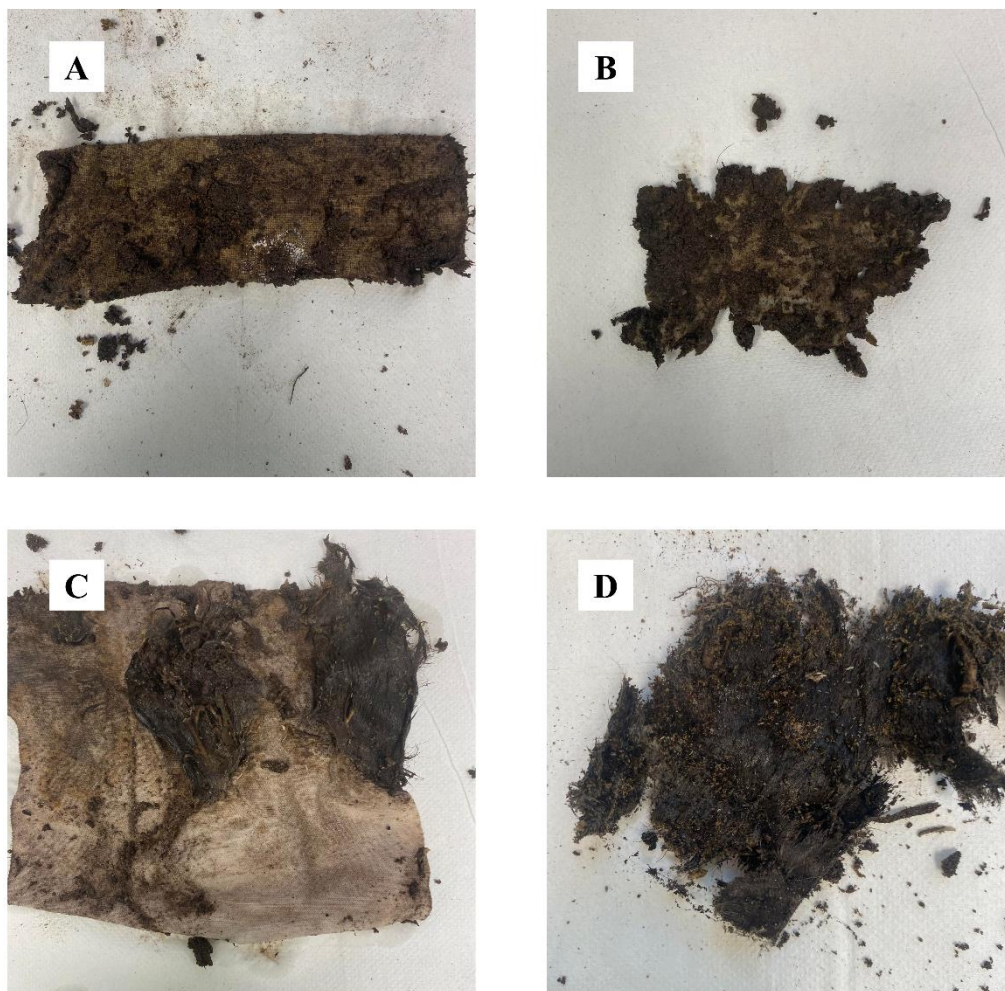


Figure 3. Remains present in microcosms after 170 days of frequent sampling: **A)** cotton (CT), **B)** viscose-wrapped *M. musculus* (VCM) **C)** polyester-wrapped *M. musculus* (PSM), **D)** unwrapped *M. musculus*.

Polyester fabric remained intact for the duration of the 170-day study irrespective of carrion presence. The resistance of these synthetic materials to enteric and exogenous microbial deterioration is well documented (4,6,22). Protection from the burial environment also provided evidence that decomposition progression in wrapped models is slowed. Polyester-wrapped mice that were in microcosms sampled throughout the study, were in advanced active decay, with some wet biomass remaining as compared to the desiccated remains identified in the unwrapped microcosms at day 170 (Figure 3D). Previous literature has inferred that clothing was incremental in retaining moisture on carrion, conferring the observed retarding of wet active decay and weight loss (12,13,27). The loss of wet biomass and impact of decay atrophy could not be taphonomically characterised as destructively sampled microcosms were not created simultaneous to each sampling intervals. However, Metcalf et al., (28) previously described 48 days as being sufficient for *M. musculus* to pass through all the decomposition stages in a semi-controlled burial simulation.

Spectral interpretation of polyester indicated deterioration in fabric integrity in response burial for 170 days, as evidenced by characteristic bands at: 720 cm^{-1} (C-H aromatic ring wagging) 1000 cm^{-1} (C-O stretching), 1245 cm^{-1} (C-O ester stretching) and 1715 cm^{-1} (C=O stretching) (4). This was observed to a greater extent in carrion-associated polyester (Figure 2). To a lesser extent, protein decomposition markers between $1650\text{--}1580\text{ cm}^{-1}$ were absorbed into the carrion-associated polyester samples. In particular, these protein indicator bands have been utilised to track proteolysis progression and PMI in porcine decomposition studies (11,23,24). Due to the non-destructive nature of the present sampling protocol these were unable to be used to monitor proteolysis through the duration of this study. Presence of triglycerides and fatty acids at 1735 cm^{-1} and 1715 cm^{-1} were not identified on the murine associated -polyester and -viscose, observed in the same porcine decomposition studies (29). However, low intensity carboxylate fatty acid salt bands detected at 1575 and 1540 cm^{-1} were identified on carrion-polyester indicating presence of lipolysis (29–31). The capturing of the aforementioned decomposition by-products would imply that some materials absorb and can impede the lateral and temporal seepage of cadaveric fluids creating a measurable CDI. However, missing evidence of both aforementioned fatty acid and protein markers in unwrapped murine decomposition microcosms may be indicative of lateral CDI formation and proxy size (32,33).

ATR-FT-IR as a tool for discriminating gravesoil

FT-IR spectra of soil were firstly investigated qualitatively to identify any patterns in spectral regions that were attributable to cadaveric by-products. The spectral regions of 3100 -2700 and 1800-1000 cm^{-1} were selected as spectral ranges of interest for decomposition and CDI products (6,8,11). Soil-only microcosm spectra ($n=3$) were characterised by little fluctuation in the spectra from day 0 to day 170 (Figure 4). Notably, shifts in O-H stretching bands and O-H bending bands at $\sim 3300 \text{ cm}^{-1}$ and $\sim 1640 \text{ cm}^{-1}$ respectively, were visible in all the spectra with changed intensity over the sampling intervals (Table 1). Although the semi-controlled fume hood locale may have induced a more desiccating environment, the microcosm soils were marked with an overall increase of internal moisture (Supplementary Figure 2). Moreover, monthly watering to mimic natural external rainfall may have accumulated in soil due to unnatural drainage, cycling capabilities and humidity generation of such types of ex situ microcosms to a real-to-life scenario. Carter et al., (9) highlighted water activity as a critical parameter governing decomposition rate in simulated juvenile rat burial. The associated water activity in gravesoil has an optimum, with extremely wet conditions promoting waterlogging and adipocere formation while extreme dehydration inducing mummification; both scenarios retard the progression of decomposition (9,34,35). Gravesoil containing *M. musculus* did not have a linear temporal increase in moisture absorption. Unwrapped murine soils recorded increased moisture absorption at $\sim 3300 \text{ cm}^{-1}$ and $\sim 1640 \text{ cm}^{-1}$ PBI=8, as well as a notable sharp bands in the C-H stretching region of symmetrical and asymmetric modes of the methylene chain (2915 and 2850 cm^{-1}) and methyl groups (2955 and 2870 cm^{-1}) indicative of lipid rich cadaveric fluid entering the soil. Lipolysis was also evidenced by carboxylate fatty acid salt bands centred at 1570 and 1545 cm^{-1} (7,34).

Metcalf et al., (28) categorised murine decomposition as: fresh stage at $\sim 0-3$ days, active decay stage at $\sim 6-20$ days (bloat days 3-9 and rupture occurring after days 6-9) and advanced decay days $\sim 20-48$. Moreover, these observations are concurrent with *M. musculus* decomposition seen in this study however, highlight contact with sterile gravesoil showing prolonged purge or active decay (36). Additional elements such as freeze thawing of the mammalian proxy and lack entomological access must also be considered in understanding the decomposition timeline seen in the current experimental design (37-39). The work carried out by Micozzi (39) reported that freezing of remains impacted all aspects of the decomposition process conferred by Roberts and Dabbs who revealed that the decomposition of frozen pigs, as assessed by accumulated degree days (ADD) and total body scoring (TBS) was significantly

slower than for fresh proxies (40). Contrastingly, Stokes, Forbes and Tibbett (41) found that freezing of *Sus scrofa* skeletal tissue did not significantly alter the decomposition timeline when in contact with soil. Concurrently, Geissenberger et al., identified that prolonged frozen storage and freeze-thaw cycles had no significant difference on decomposition behaviour and protein degradation of *S. scrofa* (42).

Table 1. Vibrational band assignment derived from PC loadings plot in simulation burial microcosms. Measured with the Cary 630 FT-IR Spectrometer (Agilent Technologies, CA, USA).

Compound	Band position (cm ⁻¹)	Band assignment
Lipids	3010 (11)	C = CH stretching
	2950 – 2850 (6,11,34)	CH ₂ wagging
	~1570, ~1540 (11,34)	C-O carboxylate
	~1370 (30)	CH ₂ wagging
Proteins	~1650, ~1550 (7)	N-H bending amide (I/II)
	1250 - 1020 (43)	C-N stretching amide (III)

The spectra collected from experimental fabric microcosms demonstrated temporal differences in band intensity to soil-only and unwrapped models (Supplementary Figure 3). When wrapped in cotton, polyester or viscose peak intensity of C-H stretching lipid methylene regions was delayed in soil until day 80, 170 and 110, respectively. In parallel volatile organic compound constituents (VOCs) that produce the characteristic smell of death such as: amines (1250 – 1020 cm⁻¹, C-N stretch) esters and carboxylic acids (1440 – 1330 cm⁻¹, O-H bending) associated with liquefaction and putrefaction of the corpse. Principal component analysis was applied to spectra obtained from all microcosms across 170 days of sampling. This facilitated visualisation of the large dataset, reducing dimensionality, and facilitating pattern recognition without loss of information (Figure 5). PC scores highlighted patterns in the simulation burial microcosms, with soils clustering based on presence or absence of unwrapped carrion (Figure 5A). Both type I and type II errors existed in gravesoil samples that can be attributed to confounding PMI or PBI data. When wrapped carrion soil samples were added to the PCA

model more type II errors were encountered with control soils (Figure 5B). However, weak temporal clustering over the 10 sampling intervals was present. Component 1 and 2 for the 3100 – 1000 cm^{-1} range accounted for over 95% of the observed variance between samples. PC loadings plot indicated that ~70% of the variance was attributed to sharp peaks at 2920 cm^{-1} and 2845 cm^{-1} and broad bands centred around 1370, 1250, 1050 cm^{-1} (Figure 6). This conferred measurable leeching of cadaveric fluids into burial soil and the impact of varying fabric on CDI progression.

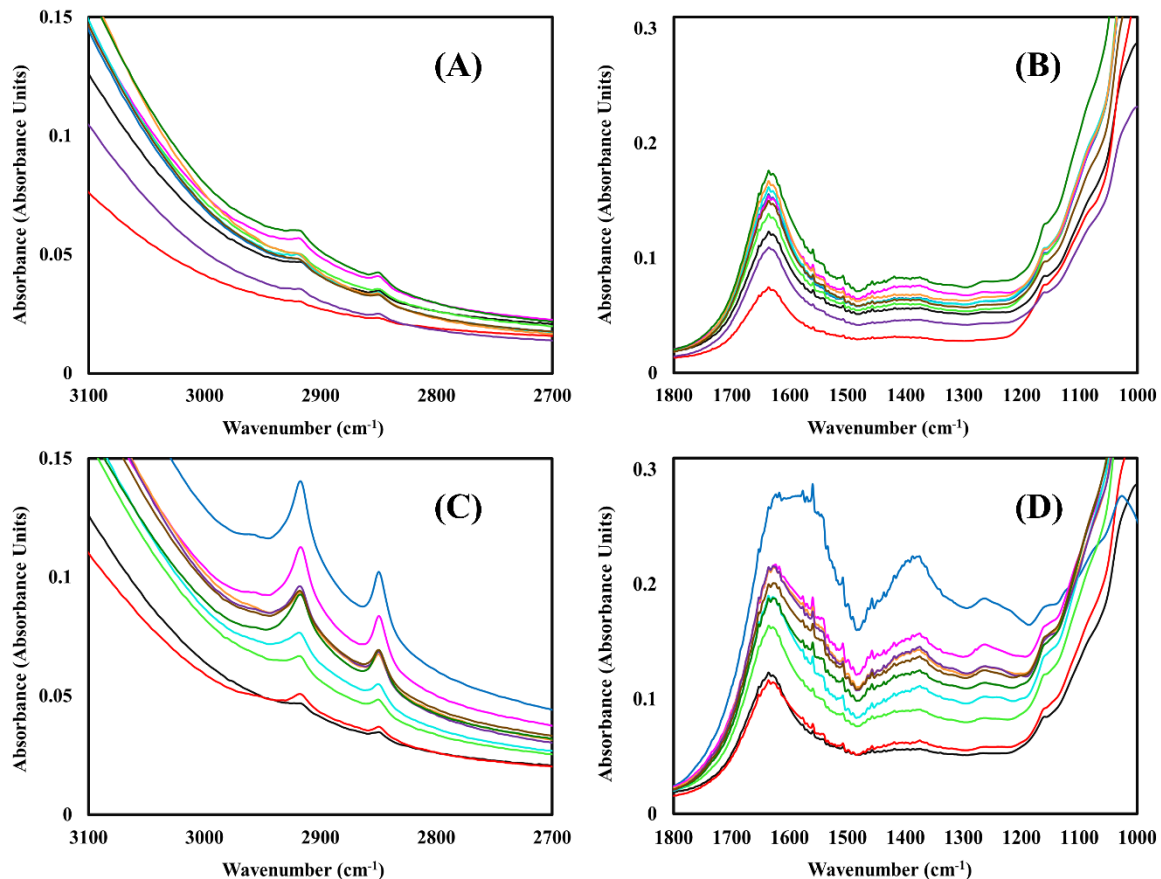


Figure 4. (A&B) FT-IR spectra of homogenised soil-only microcosm samples over the 3100 - 2700 cm^{-1} and 1800-1000 cm^{-1} regions; (C&D) FTIR spectra of homogenised unwrapped *M. musculus* microcosm samples over the 3100 -2700 cm^{-1} and 1800-1000 cm^{-1} regions; sampled on days **0, 4, 8, 16, 24, 32, 50, 80, 110** and **170**.

Conclusions

Recent advancements in spectroscopic techniques, namely FT-IR, applied to a plethora of forensic disciplines has been demonstrated in the literature. Furthermore, efforts to utilise FT-IR to gain postmortem interval estimation has proved successful in, in vitro tissue, bones and in carrion associated clothing (6,11,44,45). The application of ATR-FT-IR to soil to gain temporal decomposition information was advantageous as a non-invasive, low volume,

minimal prep forensic tool that requires little user intervention. The present study employed a simulation shallow burial study of *M. musculus* over a period of 170 days associated with cotton, polyester, and viscose. At the end of the semi-controlled ex-situ study cellulosic materials such as cotton and viscose were highly degraded when in contact with decomposing murine tissue in a burial environment. In contrast, the synthetic polyester material retained structural integrity both in the presence and absence of carrion. Spectra showed evidence of cadaveric fluid leeching into the environment, indicated by the presence of putrefactive products such as lipids, proteins, and volatile organic compounds (VOCs). Principal component analysis could discriminate soil containing carrion to control soils in a simulated laboratory-based burial microcosm in the 3100 - 1000 cm^{-1} range. Moreover, both the presence and type of fabric impeded grave and postmortem interval discrimination. Although this work provides insights into the application of ATR-FT-IR to discern gravesoil, the researchers acknowledge the inherent constraints and limitations of the study. The semi-controlled experimental design, while advantageous in minimising confounding variables, induced an unnatural burial scenario negating the interplay of key microbiological entomological, climatic and cycling conditions. Similarly, *M. musculus* and rodents are routinely utilised as human analogues not only in forensic sciences but also medical and biological research due to their similar physiology, cellular properties, anatomy, and microbiome (46,47). Their cost and size and subsequent faster decomposition allows for larger replicate cohorts and greater robustness. However, it is crucial to exercise caution when extrapolating the findings of this research to human models, particularly considering size on all aspects of decomposition and lateral (10,48,49). Looking ahead, our research provides a promising basis for utilising spectroscopy to measure temporal CDI changes. However, investigations with larger more comparable human taphonomic analogues with significant lateral soil impacts and adipocere markers should be considered next (32,50–52).

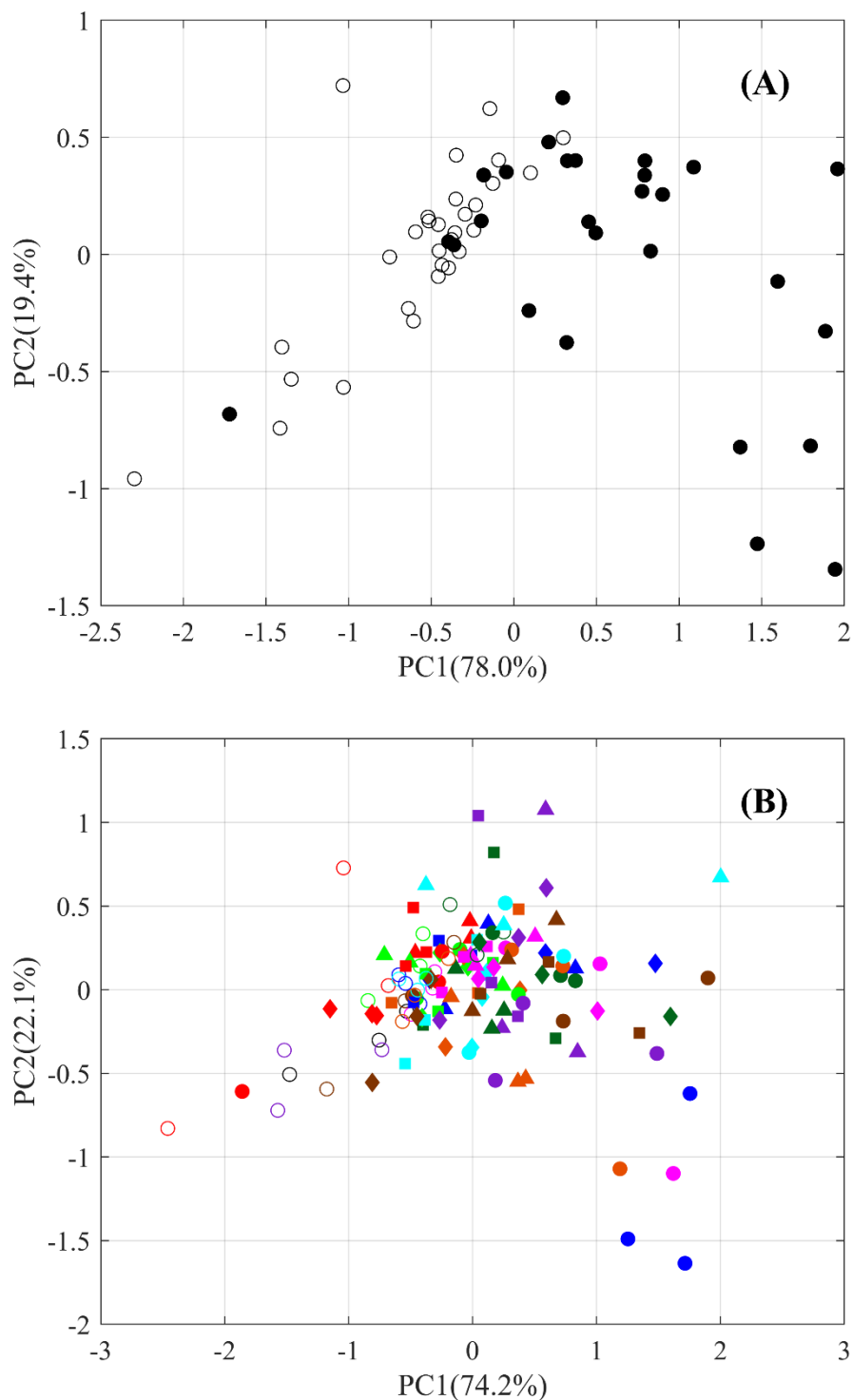


Figure 5. PC scores plot of the FT-IR spectra measured using the Cary 630 FT-IR Spectrometer (Agilent Technologies, CA, USA) in a range of 3100 – 1000 cm^{-1} range (A) Soil-only (\circ) and unwrapped murine soil samples (\bullet) (B) Soil-only microcosms (\circ), unwrapped (\bullet), cotton-wrapped (\blacktriangle), polyester-wrapped (\blacksquare) and ‘viscose’-wrapped (\blacklozenge); sampled on days 0, 4, 8, 16, 24, 32, 50, 80, 110 and 170.

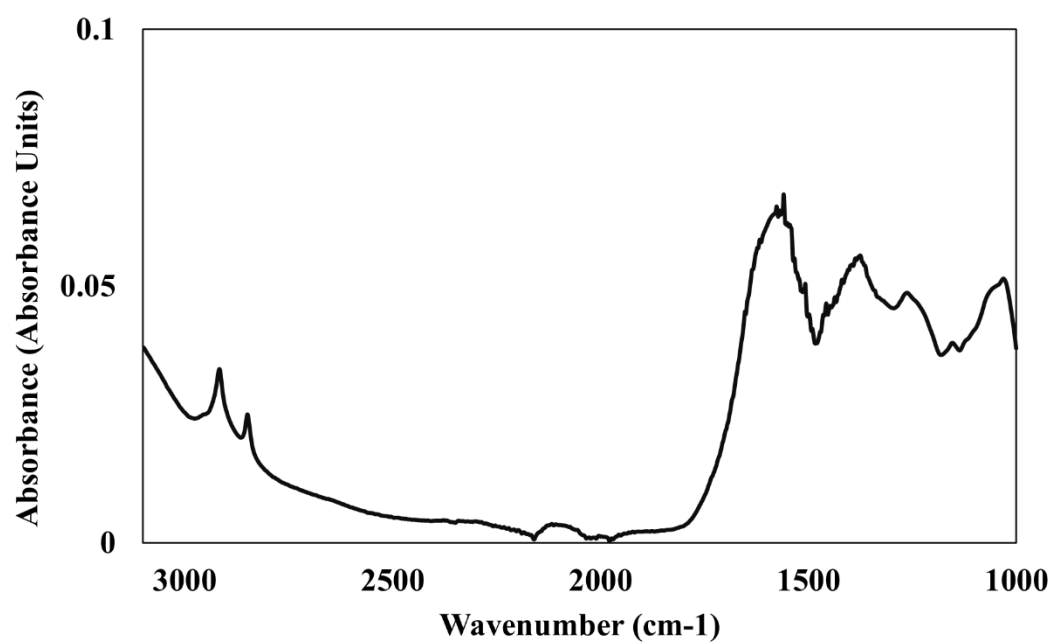


Figure 6. PC loadings plot from all soil samples, indicating component 1.

References

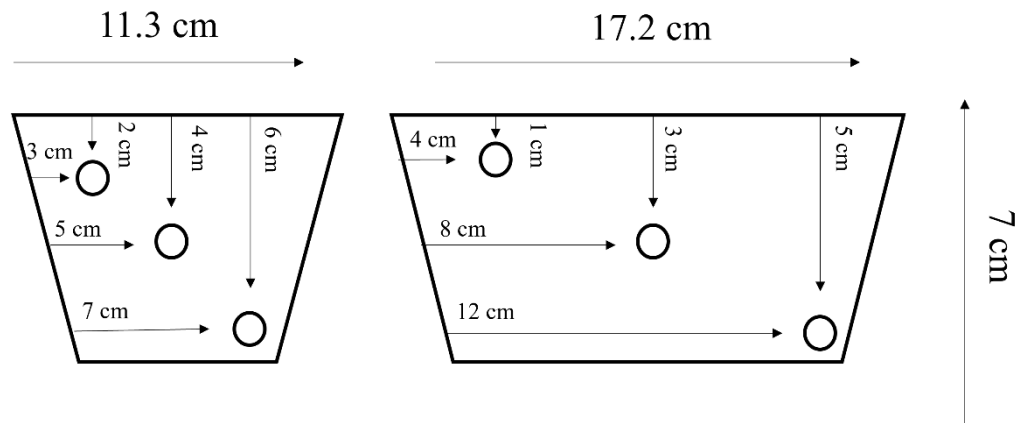
1. Scott KR, Morgan RM, Jones VJ, Cameron NG. The transferability of diatoms to clothing and the methods appropriate for their collection and analysis in forensic geoscience. *Forensic Science International*. 2014 Aug 1;241:127–37.
2. Kemp SE, Carr DJ, Kieser J, Niven BE, Taylor MC. Forensic evidence in apparel fabrics due to stab events. *Forensic Science International*. 2009 Oct 30;191(1):86–96.
3. Procter FA, Swindles GT, Barlow NLM. Examining the transfer of soils to clothing materials: Implications for forensic investigations. *Forensic Science International*. 2019 Dec 1;305:110030.
4. Ueland M, Howes JM, Forbes SL, Stuart BH. Degradation patterns of natural and synthetic textiles on a soil surface during summer and winter seasons studied using ATR-FTIR spectroscopy. *Spectrochimica Acta Part A: Molecular and Biomolecular Spectroscopy*. 2017 Oct 5;185:69–76.
5. Ueland M, Forbes SL, Stuart BH. Seasonal variation of fatty acid profiles from textiles associated with decomposing pig remains in a temperate Australian environment. *Forensic Chemistry*. 2018 Dec 1;11:120–7.
6. Ueland M, Forbes SL, Stuart BH. Understanding clothed buried remains: the analysis of decomposition fluids and their influence on clothing in model burial environments. *Forensic Sci Med Pathol*. 2019 Mar;15(1):3–12.
7. Collins S, Stuart B, Ueland M. Anatomical location dependence of human decomposition products in clothing. *Australian Journal of Forensic Sciences*. 2021 Sep 19;0(0):1–13.
8. Fancher JP, Aitkenhead-Peterson JA, Farris T, Mix K, Schwab AP, Wescott DJ, et al. An evaluation of soil chemistry in human cadaver decomposition islands: Potential for estimating postmortem interval (PMI). *Forensic Science International*. 2017 Oct 1;279:130–9.
9. Carter DO, Yellowlees D, Tibbett M. Moisture can be the dominant environmental parameter governing cadaver decomposition in soil. *Forensic Science International*. 2010 Jul 15;200(1):60–6.
10. Spicka A, Johnson R, Bushing J, Higley LG, Carter DO. Carcass mass can influence rate of decomposition and release of ninhydrin-reactive nitrogen into gravesoil. *Forensic Science International*. 2011 Jun 15;209(1):80–5.
11. Collins S, Stuart B, Ueland M. Monitoring human decomposition products collected in clothing: an infrared spectroscopy study. *Australian Journal of Forensic Sciences*. 2020 Jul 3;52(4):428–38.
12. Voss SC, Cook DF, Dadour IR. Decomposition and insect succession of clothed and unclothed carcasses in Western Australia. *Forensic Science International*. 2011 Sep 10;211(1):67–75.

13. Kelly JA, Linde TCVD, Anderson GS. The Influence of Clothing and Wrapping on Carcass Decomposition and Arthropod Succession During the Warmer Seasons in Central South Africa*. *Journal of Forensic Sciences*. 2009;54(5):1105–12.
14. Rodrigues NVS, Cardoso EM, Andrade MVO, Donnici CL, Sena MM. Analysis of seized cocaine samples by using chemometric methods and FTIR spectroscopy. *J Braz Chem Soc*. 2013 Mar;24:507–17.
15. Zapata F, de la Ossa MÁF, García-Ruiz C. Differentiation of Body Fluid Stains on Fabrics Using External Reflection Fourier Transform Infrared Spectroscopy (FT-IR) and Chemometrics. *Appl Spectrosc*. 2016 Apr;70(4):654–65.
16. Orphanou CM. The detection and discrimination of human body fluids using ATR FT-IR spectroscopy. *Forensic Science International*. 2015 Jul 1;252:e10–6.
17. Robinson LJ, Robertson AHJ, Dawson LA, Main AM. In Situ FTIR Analysis of Soils for Forensic Applications. 2015 Aug 1;30:22–30.
18. Kazarian SG, Chan KLA. Applications of ATR-FTIR spectroscopic imaging to biomedical samples. *Biochimica et Biophysica Acta (BBA) - Biomembranes*. 2006 Jul 1;1758(7):858–67.
19. Liverpool climate: Average Temperature, weather by month, Liverpool water temperature - Climate-Data.org [Internet]. [cited 2021 Jul 16]. Available from: <https://en.climate-data.org/europe/united-kingdom/england/liverpool-107/>
20. Sweiss M, Assi S, Barhoumi L, Al-Jumeily D, Watson M, Wilson M, et al. Qualitative and quantitative evaluation of microalgal biomass using portable attenuated total reflectance-Fourier transform infrared spectroscopy and machine learning analytics. *Journal of Chemical Technology & Biotechnology*. 2024;99(1):92–108.
21. Assi S, Arafat B, Lawson-Wood K, Robertson I. Authentication of Antibiotics Using Portable Near-Infrared Spectroscopy and Multivariate Data Analysis. *Appl Spectrosc*. 2021 Apr 1;75(4):434–44.
22. Sular V, Devrim G. Biodegradation Behaviour of Different Textile Fibres: Visual, Morphological, Structural Properties and Soil Analyses. *Fibres and Textiles in Eastern Europe*. 2019 Feb 28;27:100–11.
23. Ueland M, Nizio KD, Forbes SL, Stuart BH. The interactive effect of the degradation of cotton clothing and decomposition fluid production associated with decaying remains. *Forensic Science International*. 2015 Oct 1;255:56–63.
24. Lowe AC, Beresford DV, Carter DO, Gaspari F, O'Brien RC, Stuart BH, et al. The effect of soil texture on the degradation of textiles associated with buried bodies. *Forensic Science International*. 2013 Sep 10;231(1):331–9.
25. Tomšič B, Klemenčič D, Simončič B, Orel B. Influence of antimicrobial finishes on the biodeterioration of cotton and cotton/polyester fabrics: Leaching versus bio-barrier formation. *Polymer Degradation and Stability*. 2011 Jul 1;96(7):1286–96.

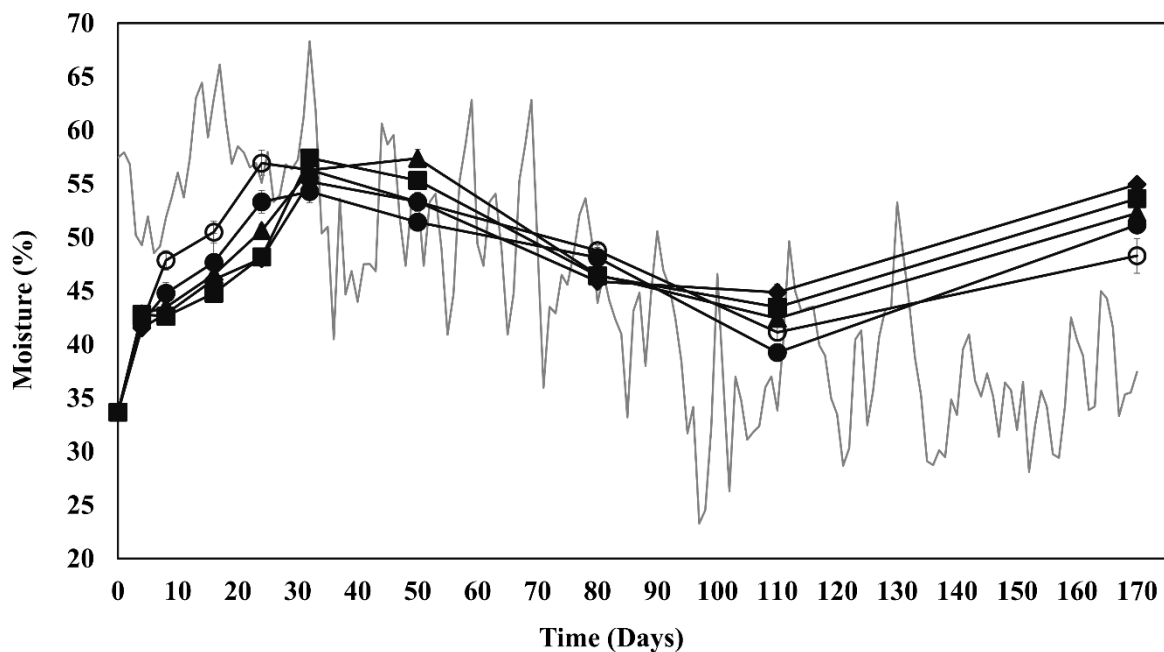
26. Smith S, Ozturk M, Frey M. Soil biodegradation of cotton fabrics treated with common finishes. *Cellulose*. 2021 May 1;28(7):4485–94.
27. Spies MJ, Finaughty DA, Friedling LJ, Gibbon VE. The effect of clothing on decomposition and vertebrate scavengers in cooler months of the temperate southwestern Cape, South Africa. *Forensic Science International*. 2020 Apr 1;309:110197.
28. Metcalf JL, Wegener Parfrey L, Gonzalez A, Lauber CL, Knights D, Ackermann G, et al. A microbial clock provides an accurate estimate of the postmortem interval in a mouse model system. Kolter R, editor. *eLife*. 2013 Oct 15;2:e01104.
29. Cassar J, Stuart B, Dent B, Notter S, Forbes S, O'Brien C, et al. A study of adipocere in soil collected from a field leaching study. *Australian Journal of Forensic Sciences*. 2011 Mar 1;43(1):3–11.
30. Forbes SL, Stuart BH, Dadour IR, Dent BB. A Preliminary Investigation of the Stages of Adipocere Formation. *J Forensic Sci*. 2004;49(3):1–9.
31. Stuart BH, Forbes S, Dent BB, Hodgson G. Studies of adipocere using diffuse reflectance infrared spectroscopy. *Vibrational Spectroscopy*. 2000 Dec 1;24(2):233–42.
32. Stokes KL, Forbes SL, Tibbett M. Human Versus Animal: Contrasting Decomposition Dynamics of Mammalian Analogues in Experimental Taphonomy. *Journal of Forensic Sciences*. 2013;58(3):583–91.
33. Ralebitso-Senior TK, Pyle MKP. Chapter 4 - Implications of the Investigative Animal Model. In: Ralebitso-Senior TK, editor. *Forensic Ecogenomics* [Internet]. Academic Press; 2018 [cited 2023 Oct 30]. p. 87–111. Available from: <https://www.sciencedirect.com/science/article/pii/B9780128093603000047>
34. Stuart BH, Craft L, Forbes SL, Dent BB. Studies of adipocere using attenuated total reflectance infrared spectroscopy. *Forens Sci Med Pathol*. 2005 Sep 1;1(3):197–201.
35. Forbes SL, Stuart BH, Dent BB. The effect of the method of burial on adipocere formation. *Forensic Science International*. 2005 Nov 10;154(1):44–52.
36. Lauber CL, Metcalf JL, Keepers K, Ackermann G, Carter DO, Knight R. Vertebrate Decomposition Is Accelerated by Soil Microbes. *Appl Environ Microbiol*. 2014 Aug 15;80(16):4920–9.
37. Bachmann J, Simmons T. The Influence of Preburial Insect Access on the Decomposition Rate. *Journal of Forensic Sciences*. 2010;55(4):893–900.
38. Pechal J, Benbow M, Tarone A, Tomberlin J. Delayed insect access alters carrion decomposition and necrophagous insect community assembly. *Ecosphere*. 2014 Apr 1;5:art45.
39. Micozzi MS. Experimental Study of Postmortem Change Under Field Conditions: Effects of Freezing, Thawing, and Mechanical Injury. *JFS*. 1986 Jul 1;31(3):953–61.

40. Roberts LG, Dabbs GR. A Taphonomic Study Exploring the Differences in Decomposition Rate and Manner between Frozen and Never Frozen Domestic Pigs (*Sus scrofa*). *J Forensic Sci.* 2015 May 1;60(3):588–94.
41. Stokes KL, Forbes SL, Tibbett M. Freezing skeletal muscle tissue does not affect its decomposition in soil: Evidence from temporal changes in tissue mass, microbial activity and soil chemistry based on excised samples. *Forensic Science International.* 2009 Jan;183(1–3):6–13.
42. Geissenberger J, Pittner S, Ehrenfellner B, Jakob L, Stoiber W, Monticelli FC, et al. Effect of temporary freezing on postmortem protein degradation patterns. *Int J Legal Med [Internet].* 2023 Jun 3 [cited 2023 Sep 29]; Available from: <https://doi.org/10.1007/s00414-023-03024-y>
43. Martínez Cortizas A, López-Costas O. Linking structural and compositional changes in archaeological human bone collagen: an FTIR-ATR approach. *Sci Rep.* 2020 Oct 21;10(1):17888.
44. Baptista A, Pedrosa M, Curate F, Ferreira MT, Marques MPM. Estimation of the post-mortem interval in human bones by infrared spectroscopy. *Int J Legal Med.* 2022 Jan 1;136(1):309–17.
45. Zhang J, Wei X, Huang J, Lin H, Deng K, Li Z, et al. Attenuated total reflectance Fourier transform infrared (ATR-FTIR) spectral prediction of postmortem interval from vitreous humor samples. *Anal Bioanal Chem.* 2018 Nov;410(29):7611–20.
46. Belk AD, Deel HL, Burcham ZM, Knight R, Carter DO, Metcalf JL. Animal models for understanding microbial decomposition of human remains. *Drug Discovery Today: Disease Models.* 2018 Jun 1;28:117–25.
47. Ralebitso-Senior TK, Pyle MKP. Chapter 4 - Implications of the Investigative Animal Model. In: Ralebitso-Senior TK, editor. *Forensic Ecogenomics [Internet]. Academic Press; 2018 [cited 2023 Oct 30]. p. 87–111. Available from: <https://www.sciencedirect.com/science/article/pii/B9780128093603000047>*
48. Weiss S, Carter DO, Metcalf JL, Knight R. Carcass mass has little influence on the structure of gravesoil microbial communities. *Int J Legal Med.* 2016 Jan;130(1):253–63.
49. Matuszewski S, Konwerski S, Frątczak K, Szafałowicz M. Effect of body mass and clothing on decomposition of pig carcasses. *Int J Legal Med.* 2014 Nov;128(6):1039–48.
50. Forbes SL, Stuart BH, Dent BB, Fenwick-Mulcahy S. Characterization of Adipocere Formation in Animal Species. *J Forensic Sci.* 2005;50(3):1–8.
51. Matuszewski S, Hall M, Moreau G, Schoenly K, Tarone A, Villet M. Pigs vs people: the use of pigs as analogues for humans in forensic entomology and taphonomy research. *International Journal of Legal Medicine.* 2020 Mar 1;134.
52. Knobel Z, Ueland M, Nizio K, Patel D, Forbes S. A comparison of human and pig decomposition rates and odour profiles in an Australian environment. *Australian Journal of Forensic Sciences.* 2018 Feb 27;51:1–16.

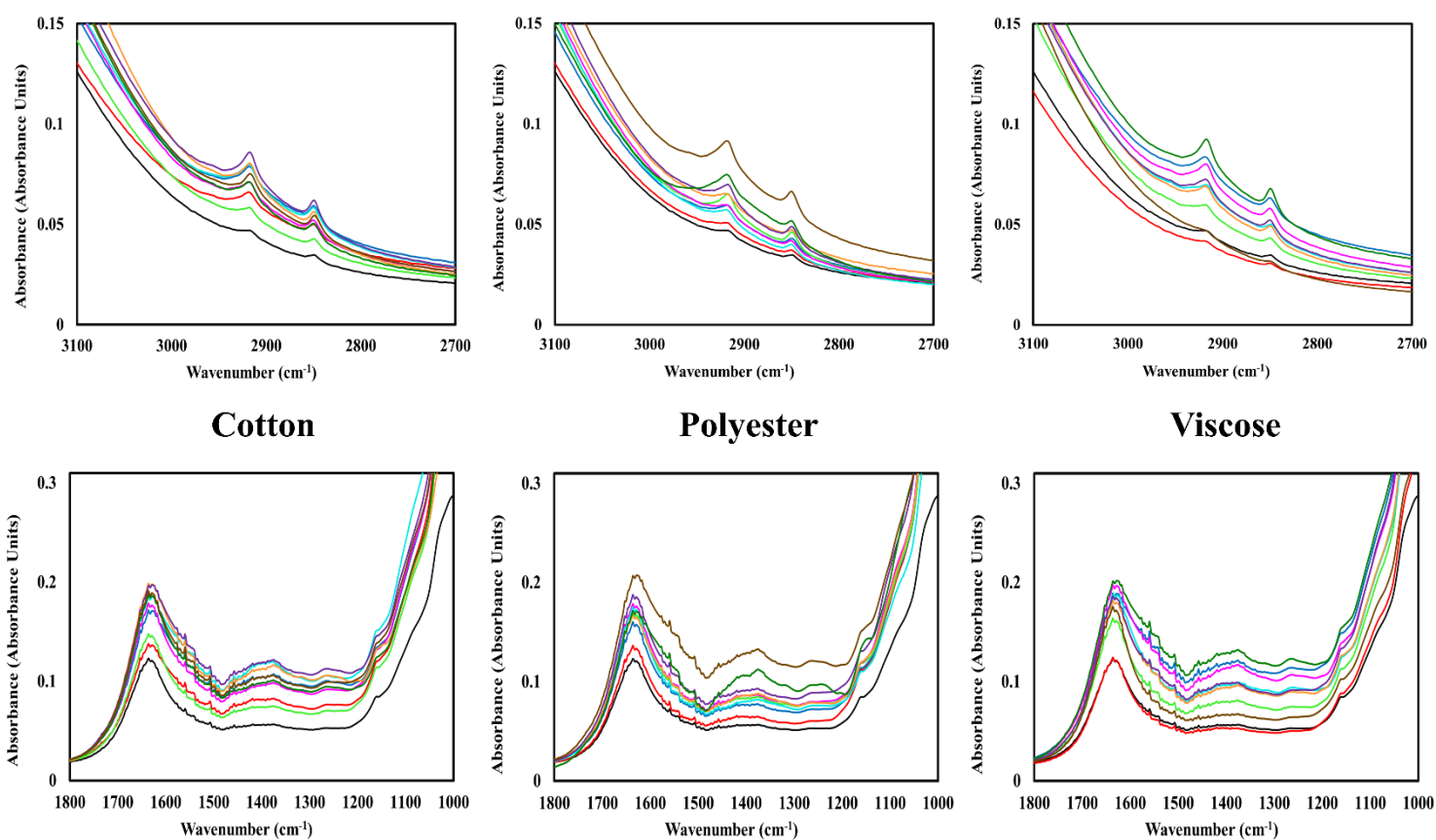
Supplementary material



Supplementary Figure 1. 1 cm perforations (n=12) created with a heated metal coring tool at: at 1 cm x 4 cm, 3 cm x 8 cm and 5 cm x 12 cm on two long sides and 2 cm x 3 cm, 4 cm x 5 cm and 6 cm x 7 cm on the alternate short sides.



Supplementary Figure 2. Changes in average (n=3) burial soil moisture (%) of the; control-only control (○) unwrapped *M. musculus* (●) and *M. musculus* wrapped in cotton (CTM; ▲), polyester (PSM; ■) and viscose (VCM; ◆) microcosm over 170 days; sampled on days 0, 4, 8, 16, 24, 32, 50, 80, 110 and 170. Average ambient external humidity (%) was recorded daily using the R-C 4H Temperature and Humidity data-loggers (Elitech Ltd., England). Bars denote Standard Deviation.



Supplementary Figure 3. FT-IR spectra of homogenised soil samples of cotton-, polyester- and viscose- wrapped *M. musculus* microcosms samples over the 3100 -2700 cm⁻¹ and 1800-1000 cm⁻¹ regions; sampled on days **0**, **4**, **8**, **16**, **24**, **32**, **50**, **80**, **110** and **170**.